ACS Catalysis

Research Article

pubs.acs.org/acscatalysis

Hydrolysis Catalysis of *Miscanthus* Xylan to Xylose Using Weak-Acid Surface Sites

Po-Wen Chung,* Alexandre Charmot, Olayinka A. Olatunji-Ojo, Kathleen A. Durkin, and Alexander Katz*

Department of Chemical and Biomolecular Engineering, University of California, Berkeley, California 94720, United States

Supporting Information

ABSTRACT: Adsorption and hydrolysis of xylan polysaccharides extracted from *Miscanthus* biomass are demonstrated, using surface-functionalized MCN (mesoporous carbon nanoparticle) materials that comprise weak-acid sites, at a pH corresponding to biomass extract. Extracted xylan polysaccharides consist of a peak molecular weight of 2008 g/mol according to GPC (gel-permeation chromatography), corresponding to approximately 15 xylose repeat units, and, a calculated length of 7 nm and radius of gyration of 2.0 nm based on molecular dynamics simulations. A highly active material for the adsorption and depolymerization of xylan is a hydrothermally treated sulfonated MCN material, which consists of 90% weak-acid sites. In spite of the large polysaccharide size relative to its 1.6 nm pore radius, this material adsorbs up to 76% of xylan strands from extract solution, at a weight loading of 29% relative to MCN. Starting with a 9.7% xylose yield in *Miscanthus* extract, this material hydrolyzes extracted xylan to xylose, and achieves a 74.1% xylose yield, compared with 24.1% yield for the background reaction in acetate buffer, at 150 °C for 4 h. Catalytic comparisons with other MCN-based materials highlight the role of confinement and weak-acid surface sites, and provide some correlation between activity and phenolic OH acid-site density. However, the lack of a directly proportional correlation between weak-acid site density and catalyzed hydrolysis rate signifies that only a fraction of weak-acid surface sites are catalytically active, and this is likely to be the sites that are present in a high local concentration on the surface, which would be consistent with previously observed trends in the hydrolysis catalysis of chemisorbed glucans on inorganic-oxide surfaces.

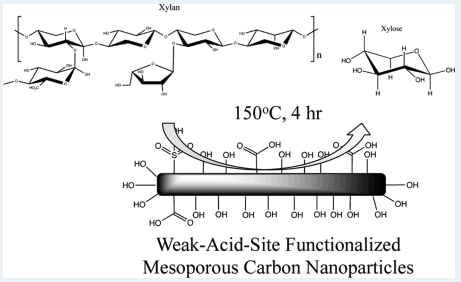

KEYWORDS: *xylan hydrolysis, mesoporous carbon, general-acid catalysis, Miscanthus biomass, depolymerization*

INTRODUCTION

The depolymerization of biomass-derived polymers into their monomeric components represents a grand challenge for enabling renewable approaches to fuels and chemicals.[1] We have recently demonstrated the hydrolysis of chemisorbed glucans that are grafted on inorganic-oxide surfaces, as an example of general-acid catalysis involving weak-acid OH defect sites in water.[2−4] We also demonstrated the rapid (transport time scale was faster than could be measured) adsorption of long-chain polysaccharides consisting of (1→4)-β-D-glucans to the interior surface of mesoporous carbon nanoparticle (MCN) materials, in spite of these polysaccharides being several-fold larger in radius of gyration than the MCN pore radius.[5] The affinity between the polysaccharide and the MCN surface was observed to increase with the molecular weight of the polymer, in a manner that was consistent with cumulative weak aromatic-carbohydrate interactions enthalpically driving adsorption, as observed previously in glycoproteins.[5] Based upon all of these data, we hypothesized that MCN materials may be able to catalyze the depolymerization of polysaccharides directly from biomass by relying exclusively on weak-acid surface sites. We rationalized such an approach to biomass-derived polysaccharide hydrolysis by the ability of the MCN to (i) rapidly adsorb polysaccharides onto the MCN internal pore space; (ii) constrain the adsorbed polysaccharides to be proximal to weak-acid sites on the MCN surface; and (iii) mechanically strain the adsorbed polysaccharide, because of its confinement within the hydrophobic environment of the internal pore space of the MCN, which favors hydrolysis as it relieves some of this strain via bond breaking of the polysaccharide into shorter segments.[4] Here, in this manuscript, we demonstrate the hydrolysis of (1→4)-β-D-xylan to xylose using weak-acid surface sites of the MCN as catalyst sites that turnover, at the mild pH of an acetate-buffered aqueous solution.

Our comparative approach hydrolyzes adsorbed xylans that have been extracted from hemicellulose of *Miscanthus* (hemicellulose represents approximately 20% by weight of the biomass), at nearly the same pH as the hemicellulose extract from raw biomass, using various surface-functionalized MCN-based materials as catalysts. This approach obviates specific-acid catalyzed hemicellulose depolymerization via hydrolysis. The latter has been studied previously[6] and has typically required an aqueous pH of below 1.5.[7−11] For instance, xylan (bagasse-derived) has been hydrolyzed to xylose at 90% conversion using

Received: October 17, 2013
Revised: November 28, 2013
Published: December 4, 2013

   dx.doi.org/10.1021/cs400939p | ACS Catal. 2014, 4, 302−310

Scheme 1. Synthesis of Functional Mesoporous Carbon Catalysts

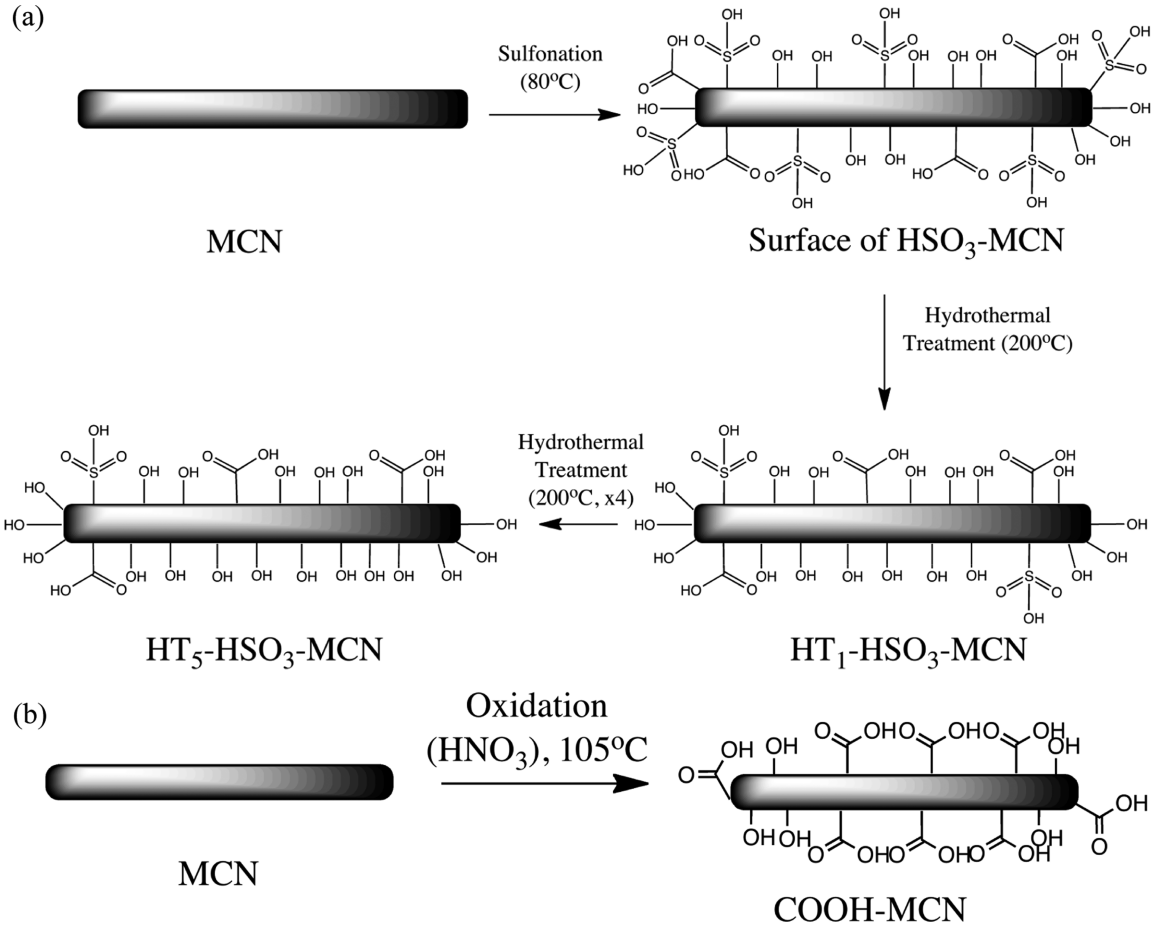

a temperature of 180 °C and pH 1.2;[9] however, the hydrolysis rate decreased significantly upon increasing aqueous pH to 2.4 at the same temperature. This is represented by a significant fraction (30%) of xylan (corn stover-derived) remaining in an oligomerized form in aqueous solution at a pH of 2.4, rather than as fully hydrolyzed xylose, even after 1 h of biomass treatment under these conditions.[10] In a recent notable and elegant example of using only weak-acid surface sites on a carbon material, in conjunction with specific-acid catalysis (0.012% aqueous HCl solution), ball-milled cellulose was hydrolyzed to glucose in a yield of up to 88%.[12] Here, in this manuscript, we compare weak-acid solid catalysts that function in the absence of added external acid in homogeneous solution, to investigate hydrolysis exclusively by weak-acid surface sites, at a buffered pH corresponding to biomass extract. Our catalysts are different from other nice examples in the literature, which combine weak-acid sites on carbon with a Lewis acidic metal (Sn(IV)) component, for conversion of trioses into alkyl lactates and lactic acid.[13]

When using solid catalysts consisting of strong-acid sites for hemicellulose depolymerization via hydrolysis, typically low monosaccharide yields of less than about 50% have been obtained.[14] We hypothesized that weak-acid catalytic sites could achieve a higher yield by potentially avoiding sequential side reactions resulting in degradation. In a recent study employing sulfonated polymer resin (Amberlyst) as catalyst, a monosaccharide yield of 75% was obtained by hydrolyzing commercially available Beechwood xylan; however, there was extensive leaching of strong-acid sites to the solution reported during hydrolysis catalysis.[15] Weak-acid sites could in principle avoid such leaching because, in contrast to strong-acid sites,[15,16] such sites are known to be much more hydrothermally stable[17] and do not leach via ion exchange in the presence of dissolved aqueous salts, which are prevalent in biomass extracts (see Supporting Information for partial list of metals present in *Miscanthus* extract solution).

Our catalyst active sites consist of weak-acid functional groups on the MCN surface. One of these is synthesized by chemical oxidation using fuming sulfuric acid followed by desulfonation via hydrothermal treatment. A sulfonated MCN material treated for five repetitive hydrothermal treatments, which is denoted as HT_5-HSO_3-MCN, consists of 1.59 mmol of total acid sites/g, with sulfonic-acid sites contributing less than 10% of the total acid sites. These sulfonic-acid sites are neutralized to yield inert salts by the buffer used during hydrolysis catalysis. Our results unequivocally demonstrate that our material HT_5-HSO_3-MCN (i) adsorbs *Miscanthus*-extracted xylan at a significant capacity consisting of up to 353 mg xylose equivalents/g; and (ii) hydrolyzes adsorbed xylan into xylose in 74% yield in acetate-buffered aqueous solution, at a pH of 3.7–4.1, 150 °C, and 4 h treatment time. The buffered conditions in the last experiment demonstrate that the observed hydrolysis catalysis of xylan into xylose is caused exclusively by weak-acid sites. This is further supported by a control material consisting of a nitric acid-treated MCN material (COOH-MCN), which lacks strong-acid (such as sulfonic acid) sites altogether and instead consists of weak-acid sites (such as carboxylic acid and phenolic OH), yet behaves similarly to HT_5-HSO_3-MCN in

dx.doi.org/10.1021/cs400939p | *ACS Catal.* 2014, 4, 302–310

hydrolysis catalysis. A comparative ATR-FTIR spectroscopy of all catalysts provides key insight into the nature of surface-functionality that are responsible for the observed weak-acid-site hydrolysis catalysis.

EXPERIMENTAL SECTION

Synthesis of Mesoporous Carbon Nanoparticles (MCN) and Functional Mesoporous Carbon Nanoparticles (HT_n-HSO_3-MCN). The synthesis of MCN material used a MCM-48-type mesoporous silica nanoparticle (MSN) material as the structure-directing template via a modified Stöber approach, as described previously.[18,19] The functional MCN material (HSO_3-MCN) was synthesized by using fuming H_2SO_4 (20% of SO_3) solution as an oxidizing agent.[20] MCN materials (1.2 g) were treated in fuming sulfuric acid solution (80 mL) in a round-bottom flask (50 mL), and the mixture was heated under nitrogen at 80 °C for 24 h. After reaction, the as-synthesized functional MCNs were collected via filtration and washed with copious amounts of water. The as-synthesized MCN materials (1.2 g) were Soxhlet extracted with 250 mL of water for a period of 3 h, and this extraction procedure was repeated four times. Afterward, HSO_3-MCNs (0.5 g) were placed in an autoclave in the presence of water (15 mL), and hydrothermal treatment was conducted at 200 °C and autogenous pressure for 3 h.[21] The material after hydrothermal treatment (HT_1-HSO_3-MCN) was collected by filtration and washed by the aforementioned Soxhlet extraction procedure. Such hydrothermal treatment was repeated for four more repetitions to synthesize HT_5-HSO_3-MCN (and, in general, for a total of $(n-1)$ more repetitions to synthesize HT_n-HSO_3-MCN) as shown in Scheme 1. To monitor the sulfate leached from the carbon surface after the hydrothermal treatment above, 1 mL of $BaCl_2$ (1 M) solution was mixed with 1 mL of the filtrate following hydrothermal treatment. Because the solubility product (K_{sp}) of barium sulfate is 1.1×10^{-10}, a white precipitate is observed if there is even trace sulfate (ppb level) present in solution. In general, there was no white precipitate observed after the fourth hydrothermal treatment. To synthesize COOH-MCN, MCNs (300 mg) were placed in a 100 mL round-bottom flask with 30 mL of nitric acid (1M), and the solution was refluxed at 105 °C for 1.5 h. This was then followed by hot filtration, a wash with copious of water, and Soxhlet extraction with water. MCNs and functional MCNs were completely dried under vacuum before further adsorption and hydrolysis reaction.

Extraction of Xylan Solution from *Miscanthus*. Dry *Miscanthus* (3 g, 0.12 mm in particle size) was placed in a microwave canister and added to 30 g of Mill-Q water. A microwave reactor was programed to heat up to a designated temperature of 190 °C and a specified residence time of 10 min. After reaction, the canister was cooled in an ice bath, the solution was filtered using a glass-fiber filter, and the collected *Miscanthus* was washed with 30 g Mill-Q water. The xylan in the filtrate was subsequently determined by NREL hydrolysis[22] and analyzed by HPLC. A typical procedure was to acidify the filtrate (1 mL) using 35.8 μL of 72 wt % H_2SO_4, and follow the standard NREL hydrolysis protocol to subsequently determine the mass of xylan recovered from *Miscanthus*.

Adsorption of Xylans on MCN. The xylan extract derived from *Miscanthus* (1.5 mL) was treated with 8 mg (at concentrated region) or 25 mg (at diluted region) of MCN material at room temperature for 30 min. The quantity of adsorbed xylans was determined by filtration and analysis of the filtrate via HPLC. This was performed by first hydrolyzing xylans in the filtrate to xylose using standard NREL hydrolysis conditions.

Hydrolysis of Xylan Using HT_n-HSO_3-MCN. The xylan extract derived from *Miscanthus* (1 mL) was treated with 10 mg of HT_n-HSO_3-MCN material in a crimped vial at 150 °C for 4 h. For the hydrolysis in buffer solution, the xylan extract (6 mL) was mixed with sodium acetate buffer solution (0.02 M, 2 mL) before being treated with HT_n-HSO_3-MCN material. After reaction, a Speedisk column (J. T. Baker 8163-04, silica base) was employed for separation of solid HT_n-HSO_3-MCN via filtration, and the filtered HT_n-HSO_3-MCN was subsequently washed with 4 mL of warm water (85−90 °C). The xylose concentration in the filtrate was analyzed via HPLC.

Size-Exclusion Chromatography/Gel Permeation Chromatography (SEC/GPC). Xylan extract (100 μL) was dispersed in 0.9 mL of 0.5 wt % LiCl/DMAc, and the solution was filtered using a 0.2 μM Nylon syringe filter prior to measurement. SEC/GPC was performed on a Polymer Laboratories PLGPC-50 instrument, equipped with a refractive index concentration detector (RI). Separation was performed on a two-column series consisting of PLGEL-Mesopore 300 × 7.5 mm preceded by a Mesopore guard column 5 μM particles 50 × 7.5 mm (Polymer Laboratories). The mobile phase consisted of 0.5 wt % LiCl in DMAc, and was used at a flow rate of 0.9 mL/min. The oven temperature was set to 50 °C. Calibration data were collected for a series of standards including D-(+)-glucose (Mp = 180), and polysaccharides consisting of: Stachyose (Mp = 667, from Varian) and pullulan polysaccharides (Mp = 5900; 11100; 21100; 47100; 107000; 200000; 375000; 708000, from Varian). The injection volume was set to 100 μL, and the run time was set to 75 min. Data acquisition and analysis was performed using Cirrus software.

Characterization of Mesoporous Carbon Materials. Nitrogen physisorption isotherms were measured at liquid nitrogen temperature (77 K) using a Micromeritics ASAP 2020 volumetric adsorption analyzer. The Brunauer−Emmett−Teller (BET) equation was used to calculate the internal surface area from adsorption data obtained at P/P_0 between 0.05 and 0.2. The total volume of micropores and mesopores was calculated from the amount of nitrogen adsorbed at $P/P_0 = 0.95$. The pore-size distributions (PSD) were calculated by analyzing the adsorption branch of the nitrogen physisorption isotherm using the Barret−Joyner−Halenda (BJH) method. Elemental analysis was employed to characterize the amounts of sulfur on MCNs by Intertek Pharmaceutical Service. The number density of total acid sites immobilized on functional MCNs was determined by acid−base back-titration.[23,24] Functional MCNs (50 mg) were treated with 0.01 N NaOH aqueous solution (15 mL) and equilibrated for a period of 2 h. After equilibration, the solids were collected via filtration and washed with 10 mL of Mill-Q water. The collected filtrate was titrated with 0.01 N HCl using phenolphthalein as indicator. Raman spectroscopy was analyzed using LabRAM IR confocal Raman device, and the green laser used for measurement was DPSS C.W. 532.1 nm laser with a power of 50 mW. The hole was set as 1000 μm, and the slit was set as 100 μm. ATR-FTIR analysis was conducted out using a Nicolet 6700 equipped with an ATR cell from Thermo Scientific.

RESULTS AND DISCUSSION

A set of functionalized MCN surfaces was synthesized starting withwet-chemical oxidation using fuming sulfuric acid; in

dx.doi.org/10.1021/cs400939p | ACS Catal. 2014, 4, 302−310

general, such oxidation synthesizes carbon surfaces that are functionalized with sulfonic acid and carboxylic acid, as well as phenolic functional groups.[20] The MCN material resulting from the oxidation treatment (HSO_3-MCN) was found to consist of 0.4 mmol of sulfur/g, which represents the density of sulfonic acid functionality on the carbon surface. Typically, acid−base back-titration is used to measure the total number of acidic groups on a carbon material,[23,24] since the base typically used, NaOH, neutralizes all acid groups on the surface (consisting of sulfonic acid, carboxylic acid, and phenolic OH functional groups). The number density of total acid sites as measured via acid−base back-titration on HSO_3-MCN was 1.38 mmol/g for HSO_3-MCN material. This suggests that almost 1 mmol/g of the total acid site density originates from weak-acid sites (carboxylic acid and phenolic OH functional groups) in HSO_3-MCN, which is a 61% increase from 0.62 mmol/g of weak-acid sites for the original MCN material. This data is consistent with the oxidation treatment increasing both number densities of strong-acid (sulfonic) sites as well as weak-acid sites on the surface. It also decreased the surface area and pore volume by 20%, which is typical when using similar procedures reported for other materials and is attributed to destructive oxidation of the carbon material.[17] We investigated all MCN-based materials using Raman spectroscopy, and they all exhibit distinct G (at 1580 cm^{-1}) and D (at 1350 cm^{-1}) bands corresponding to the E_{2g} G mode and the A_{1g} D mode, respectively (see Supporting Information).[25]

To remove acid sites that are hydrolytically unstable, such as a certain fraction of sulfonic-acid sites on HSO_3-MCN, hydrothermal treatment using water at 200 °C was employed, so as to synthesize HT_1-HSO_3-MCN (HT represents a hydrothermally heat-treated material),[21] in which the number density of sulfonic-acid sites was reduced to 0.22 mmol/g. The total acid-site number density as measured using acid−base back-titration (1.36 mmol/g) as well as the surface area and pore volume in Table 1 remained almost unchanged when comparing hydrothermally treated materials and HSO_3-MCN. This result is unexpected because the hydrothermal cleavage of the S−C bond in surface-functionalized sulfonic-acid MCN materials should in principle synthesize a nonacidic and aprotic site on carbon, according to the same type of reaction as observed, for example, with benzenesulfonic acid, which leads to benzene and sulfuric acid as product. Our results instead suggest a slight increase in the number density of weak-acid sites on the carbon surface with the hydrothermal treatment above. We repeated this treatment for four additional cycles, as summarized in Table 1, and by doing so further reduced the number density of sulfonic-acid sites while slightly increasing that of weak-acid sites on the carbon surface. A $BaCl_2$-assay was used to qualitatively monitor sulfonic-acid leaching from the material in between successive hydrothermal treatments, in synthesizing materials HT_n-HSO_3-MCN where n varies from 1 to 5, via formation of a characteristic white $BaSO_4$ precipitate. HT_4-HSO_3-MCN was the first in this series of materials not to contain a detectable trace of precipitate when using this sensitive assay, suggesting that sulfonic acid leaching had virtually ceased by the fourth cycle. The final resulting material, HT_5-HSO_3-MCN, possessed only 0.13 mmol sulfonic acid/g, which is less than 10% of the total acid-site number density of 1.59 mmol/g as measured by acid−base back-titration for HT_5-HSO_3-MCN. The weak-acid site number density in HT_5-HSO_3-MCN is 2.4-fold higher when compared with the original MCN material (i.e., before oxidation and hydrothermal treatments).

Table 1. Surface Properties of MCN and Surface-Functionalized MCN Catalysts

catalyst	surface area S_{BET} (m^2/g)	pore volume (cm^3/g)	sulfur[a] (mmol/g)	acid sites[b] (mmol/g)
MCN	2131	1.4	-	0.62
HSO_3-MCN	1701	1.1	0.40	1.38
HT_1-HSO_3-MCN	1701	1.1	0.22	1.36
HT_5-HSO3-MCN	1698	1.1	0.13	1.59
COOH-MCN	1644	1.0	-	1.8

[a]Sulfur content was determined by elemental analysis. [b]Acid sites were determined by acid−base back-titration.

We chose *Miscanthus* as the source for lignocellulosic biomass, since this is considered a promising feedstock for the production of biofuels and related value-added chemicals.[26] *Miscanthus* consists of three major biopolymers (cellulose, hemicellulose, and lignin), with an average composition comprising 42.2 wt % glucan, 20.6 wt % Klason lignin, 19.9 wt % xylan, 6.61 wt % extractives, 2.72 wt % acetate, 1.73 wt % arabinan, 3.05 wt % total ash, and 2.01 wt % ash.[27] Though some breakdown of the xylan polysaccharides is expected to inevitably occur under the hydrothermal conditions of extraction, we intentionally tried to choose extraction conditions that preserve the integrity of xylan polysaccharide as found in the original raw biomass. We reasoned that such a longer-chain xylan will adsorb with greater affinity to the MCN material, because of a greater number of carbohydrate-aromatic interactions per strand, as observed previously with glucans.[5] Such a greater adsorption affinity ultimately enables use of more dilute extract solutions, since adsorption saturation occurs at lower concentrations. When adsorbed, the longer-chain xylan is expected to be confined and strained to a higher degree within the MCN pore, which should favor its hydrolysis and

Scheme 2. Closure of the Material Balance between Pretreated *Miscanthus* and Xylan Extract

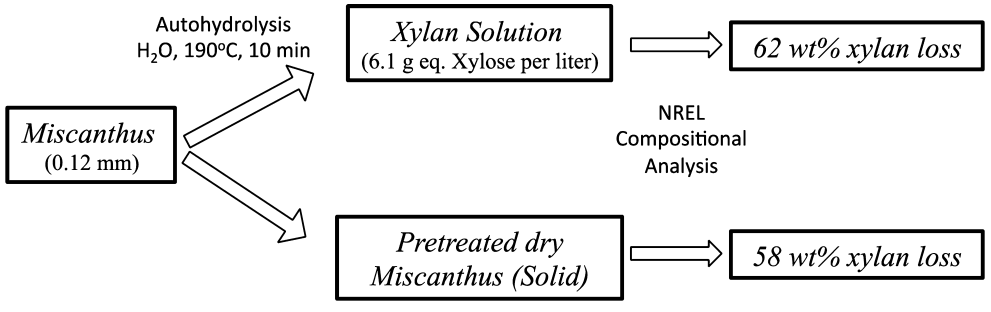

dx.doi.org/10.1021/cs400939p | ACS Catal. 2014, 4, 302−310

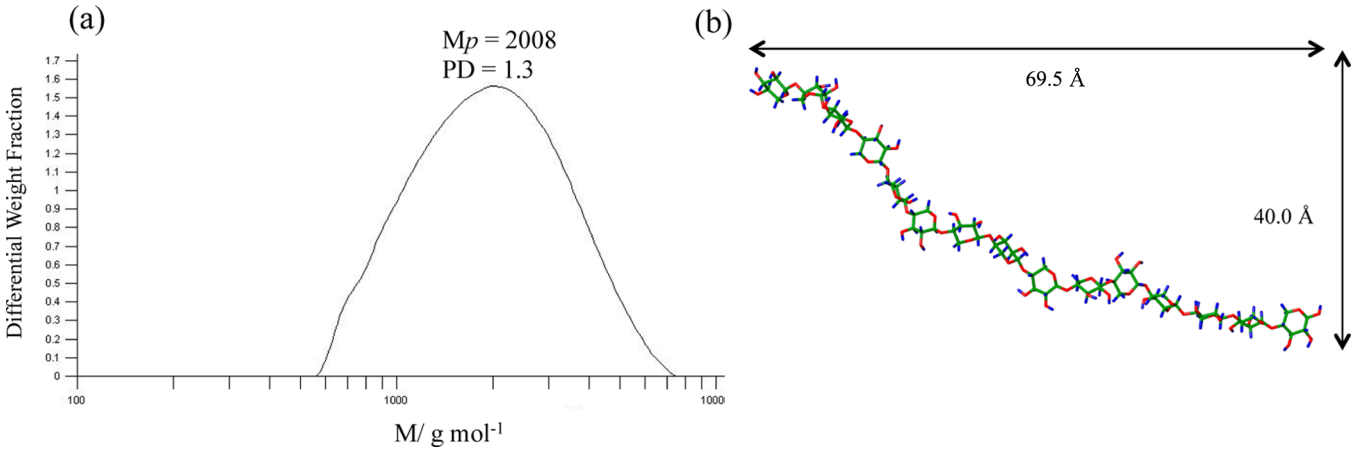

Figure 1. (a) Major molecular weight distribution for xylan extract from *Miscanthus* (Mp represents peak average molecular weight (g/mol), and PD represents polydispersity index) measured by GPC. (b) Molecular dynamics simulation in explicitly solvated water after 10 ns of the 15-mer (1 → 4)-*β*-D-xylan polysaccharide represented by Mp in (a). The calculated radius of gyration is 2.05 nm. Water molecules are excluded for clarity.

concomitant release of this strain, when activated for hydrolysis via weak-acid surface sites.[4]

We extracted xylan from dry *Miscanthus* using an autohydrolysis pretreatment and Mill-Q water that is heated in a microwave reactor. We thus treated dry *Miscanthus* in water by rapidly heating up to a temperature of 190 °C within a two-minute time frame, and holding at that temperature (soaking) for ten minutes. This achieved a high ratio of polymeric xylan over monomer in the extract solution. The polymer/monomer weight ratio in the extract was measured to be 8.5 (i.e., 88% of xylan in the filtrate consists of two or more repeat units), with a measured xylose concentration in the extract of 0.6 g/L. Based on HPLC data, this procedure extracts 62 wt % of the xylan from the dry *Miscanthus* biomass, resulting in a concentration of xylan filtrate extracted from *Miscanthus* of 6.1 g of xylose equivalents per liter. Closure of the material balance was performed by analyzing the *Miscanthus* solids composition before and after pretreatment, as shown in Scheme 2. Size-exclusion chromatography/gel permeation chromatography (SEC/GPC) was used to further investigate the degree of polymerization of xylan that was extracted from *Miscanthus* in the hot-water treatment described above, and these results are shown in Figure 1a. The peak-average molecular weight (M*p*) of extracted xylan was 2008 g/mol with a polydispersity (PD) of 1.3 and a weight-average molecular weight (M*w*) of 2197 g/mol, corresponding to a peak-average xylan consisiting of 15 xylose repeat units, within the extracted polysaccharides. Molecular dynamics simulations modeled the size of this peak-average xylan strand in aqueous solution, using explicit water molecules, and these results are represented in Figure 1b. This xylan consists of a 6.95 nm long strand on one of its ends and a radius of gyration of 2.05 nm. We expect that the extracted xylans are strained upon adsorption to the MCN pore (1.6 nm radius) because the curvature of the MCN porosity is considerably smaller than the strand length and was previously shown to be commensurate with the length scale of a cellotetraose (<0.8 nm).[5]

Leveraging on our previous demonstration that MCN material adsorbs long-chain polysaccharides consisting of glucans, where a large fraction of the adsorbed polysaccharide distribution had a larger radius of gyration than the MCN pore radius,[5] we hypothesized that xylan polysaccharides could also adsorb to MCN, using similar aromatic-carbohydrate interactions. To investigate this possibility, the xylan extract derived from *Miscanthus* described above was equilibrated with MCN material at room temperature, and the quantity of xylan adsorbed was determined by analyzing filtrate via HPLC, by hydrolyzing remaining xylans in the filtrate to xylose using standard NREL hydrolysis conditions.

Results from xylan adsorption experiments on various materials are summarized in Table 2. Untreated MCN adsorbs a maximum of 377 mg xylose equivalents/g when treated with excess xylan in solution. This is slightly larger than the mass uptake of polysaccharides when adsorbing long-chain glucans on similar MCN materials. Material HSO_3-MCN adsorbed 248 mg xylose equivalents/g under similar conditions, which represents a slight decrease in the amount of adsorbed xylan relative to untreated MCN. After further hydrothermal treatment, HT_1-HSO_3-MCN and HT_5-HSO_3-MCN adsorb 330 mg xylose equivalents/g and 353 mg xylose equivalents/g, respectively, under similar conditions, which are comparable to the adsorption capacity of untreated MCN. When operating at a slightly lower adsorption capacity corresponding to 292 mg xylose equivalents/g, HT_5-HSO_3-MCN adsorbs 76% of the xylose content in solution, as shown in Table 2. These data show that *Miscanthus*-extracted xylans adsorb to either MCN or surface-functionalized MCN materials in quantities that are either similar to or slightly exceed those previously reported for glucans.[5]

Table 2. Adsorption Data of Xylan on MCN Catalysts

samples	percentage of adsorbed xylan (%)	mass of adsorbent (mg)	xylan solution volume (mL)	xylan adsorbed on carbon materials (mg $_{\text{xylose eq}}$ /g carbon)
(A) MCN	30.1	7.7	1.5	377
(B) MCN	82.4	25.2	1.5	316
(C) HSO_3-MCN	19.5	7.6	1.5	248
(D) HSO_3-MCN	72.4	24.8	1.5	282
(E) HT_1-HSO_3-MCN	25.3	7.4	1.5	330
(F) HT_1-HSO_3-MCN	75.5	25.4	1.5	287
(G) HT_5-HSO_3-MCN	28.1	7.7	1.5	353
(H) HT_5-HSO_3-MCN	75.9	25.1	1.5	292

dx.doi.org/10.1021/cs400939p | *ACS Catal.* 2014, 4, 302−310

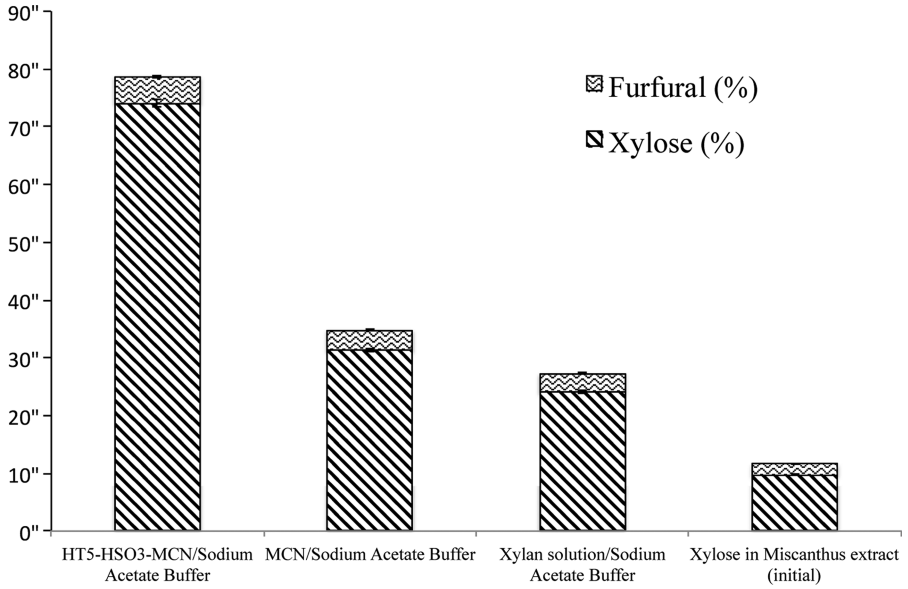

Figure 2. Hydrolysis yield of xylan using mesoporous carbon catalysts in the presence of sodium acetate buffer, which is expressed on the basis of total xylose equivalents content of the *Miscanthus* extract. This extract contains a slight amount of xylose and furfural as represented by the rightmost bar.

Hydrolysis of xylan using MCN catalysts was investigated using functionalized MCNs consisting of HT_n-HSO_3-MCN (10 mg) and xylan filtrate (1 mL), at 150 °C for 4 h. We buffered the medium during hydrolysis catalysis using a sodium acetate/acetic acid buffer, to control the strength of acid sites both on the solid MCN surface as well as in (homogeneous) solution to be comparable with the strength of acids (i.e., acetic acid) native to biomass-extract solution. The latter had a pH of 3.9 and significantly lower than the pH of 7.0 of the water used for extraction, because of released acetate during hydrothermal biomass treatment, since acetate is typically released from biomass containing hemicellulose with a xylan backbone.[28] The particular buffer composition used corresponds to a pH of 4.1 (with a typical working sodium acetate/acetic acid buffer range being 3.6 < pH < 5.6). Using this buffer also ensures at least partial protonation of carboxylic (pK_a 4.76) and phenolic (pK_a 10.0) functional groups as weak-acid sites on the MCN surface, while ensuring deprotonation of the much stronger sulfonic-acid sites on the surface, to yield catalytically inert sodium sulfonate salts. Thus, by conducting the hydrolysis reaction in a buffered solution, the catalytic effect of the minority of strong sulfonic-acid sites from the majority of weak-acid sites that are present in HT_n-HSO_3-MCN materials can be rigorously eliminated. This would be impossible to do in the absence of a buffered solution during hydrolysis reaction, since even though strong-acid sites are present in smaller number density on the surface in HT_5-HSO_3-MCN, they may be more catalytically active per site via specific-acid catalyzed hydrolysis.

Catalysis results in sodium acetate buffer solution are shown in Figure 2. Catalyst HT_5-HSO_3-MCN yields 74.1% xylose, which is significantly higher than either untreated MCN or buffered xylan extract solution (containing no catalyst) as controls at the same pH of 3.7−4.1. The latter control had a xylose yield of 24.1% whereas the former control had a xylose yield of 31.3%. The similarity of the xylose yield in both of these controls rules out the effect of confinement alone as being responsible for hydrolysis catalysis, since, if this were the case, the untreated MCN would be more significantly departed from the acetate-buffer control (and would have a similar activity to HT_5-HSO_3-MCN, vide supra). In all three cases, there is some furfural remaining after reaction (xylose to furfural ratio is 16 for HT_5-HSO_3-MCN and is about 8 for the other two systems), and the pH decreases slightly during the course of reaction (Figure 2) presumably because of formation of either acidic degradation side products (from observed furfural) or additional hydrolytic release of acetate from the xylan polysaccharide. The observed activity of the buffered xylan extract solution is consistent with previously reported xylan hydrolysis activity, when considering the xylose content of the initial (before hydrolysis reaction) extract solution, which corresponds to 9.7% of total xylose in Figure 2.[7−11]

The catalytic nature of xylose hydrolysis for data in Figure 2 is exemplified by the fact that each acid site in HT_5-HSO_3-MCN has undergone several turnovers (i.e., has hydrolyzed multiple glycosidic bonds). When the hydrolysis reaction is conducted in the absence of buffer, for extract alone containing no catalyst, untreated MCN catalyst, and HT_5-HSO_3-MCN, the hydrolysis activity and xylose yield increases slightly because of the lower pH attained without buffer, upon release of acidic degradation reaction products and/or acetate release (as shown in Supporting Information, Figure S1). A representative example is catalytic material HT_5-HSO_3-MCN: its xylose yield increased to 77%—a 3% increase over acetate-buffered conditions. When comparing the xylose yield of catalysts using unbuffered xylan extract, functionalized-MCN materials HT_5-HSO_3-MCN, HT_1-HSO_3-MCN, and HSO_3-MCN are all similar. This result is surprising given that the catalytic activity of HT_5-HSO_3-MCN relies on weak-acid sites as described above, whereas material HSO_3-MCN is expected to leach sulfonic acid during hydrolysis catalysis, as reported in related sulfonated materials.[15] This underscores the fact that yields of hydrolysis products can be equally high when using either leachable sulfonic-acid surface sites versus hydrothermally stable weak-acid surface sites.

The observed increase in xylose yield when comparing HT_5-HSO_3-MCN and MCN in Figure 2 cannot be explained by

dx.doi.org/10.1021/cs400939p | *ACS Catal.* 2014, 4, 302−310

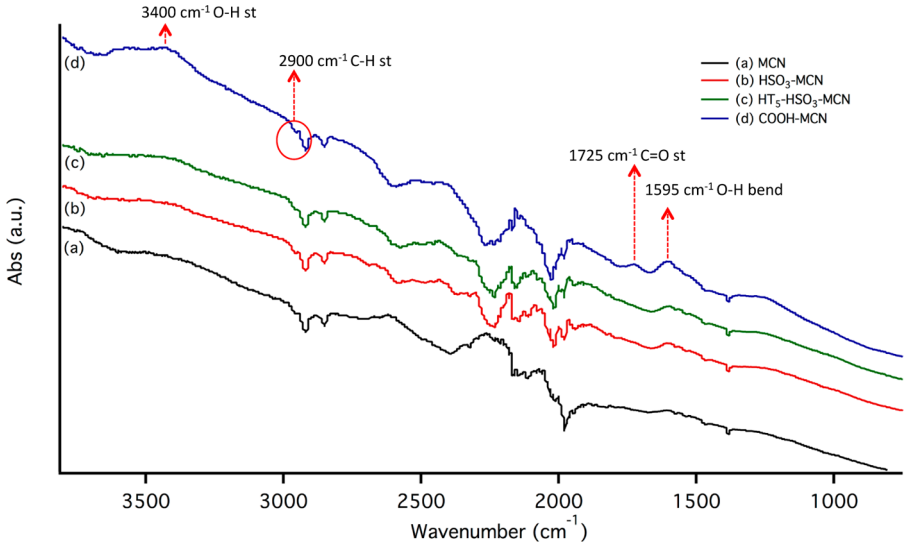

Figure 3. FTIR spectra of (a) MCN (black), (b) HSO_3-MCN (red), (c) HT_5-HSO_3-MCN (green), and (d) COOH-MCN (blue). Regions corresponding to O−H, C−H, and C═O stretches are highlighted, alongside the band for O−H bending.

either the presence of a small number of residual sulfonic-acid sites (because of their neutralization by buffer; vide infra) or the contributions from solution, as shown by the acetate-buffer control. However, the observed increase in xylose yield when using HT_5-HSO_3-MCN is inconsistent with its density of weak-acid sites relative to MCN. The latter has a reduced weak-acid site density (per gram basis) of 2.4-fold relative to the former according to data in Table 1; however, the former exhibited a more than 7-fold increased hydrolysis rate over background (per gram basis) relative to the latter in Figure 2. This demonstrates a correlation between phenolic OH weak-acid site density and hydrolysis catalytic activity, but it also suggests that factors besides total number of weak-acid functional groups are controlling, such as the organization or positioning of these sites on the surface. Reaction kinetics are consistent with a uniform rate of xylose release during the hydrolysis reaction (Supporting Information, Figure S9).

We further ruled out any possible role of residual sulfonic-acid sites by two experiments. First, we performed an acetate-buffer pretreatment of the HT_5-HSO_3-MCN and HSO_3-MCN materials by separately treating 25 mg of each MCN-based material with 25 mL of 0.02 M sodium acetate buffer (under vortex for 1 h and subsequently filtering, washing with 5 mL of deionized water, and drying), before treatment with xylan-extract and acetate buffer solutions, and subsequent hydrolysis reaction in the acetate-buffered xylan extract. We compared the results with and without buffer pretreatment for strong- and weak-acid solid catalysts, and these are represented in the Supporting Information, Figure S10. Acetate-buffer-pretreated HSO_3-MCN was significantly deactivated relative to the same material without the buffer pretreatment, to the point where its activity for xylan hydrolysis was similar to a control consisting of the original MCN (i.e., no evidence of sulfonic-acid catalysis in HSO_3-MCN after buffer pretreatment). This experiment demonstrates that the buffer pretreatment poisons strong acid sites. In stark contrast, when comparing acetate-buffer-pretreated HT_5-HSO_3-MCN with the same material without buffer pretreatment, there was only a slight observed decrease in xylose yield in Figure S10 of the Supporting Information upon buffer pretreatment. This minor decrease in activity is attributable to the small fraction of residual sulfonic acid sites in HT_5-HSO_3-MCN (vide supra). Second, we synthesized COOH-MCN catalyst, using nitric-acid treatment of MCN, which is known in the literature to synthesize a carboxylated catalyst, which consists of a combination of carboxylic acid and possibly some phenolic OH-functional groups on the MCN surface via oxidation but notably lacks acid sites of the strength of anchored sulfonic acids.[17,29] In buffer solution, the resulting catalyst COOH-MCN exhibits an activity that is similar to HT_5-HSO_3-MCN, according to data in Figure 2. This result further demonstrates xylan hydrolysis-catalysis activity solely by weak-acid (carboxylic and phenolic) surface sites.

The catalytic activity of COOH-MCN and MCN did not change significantly upon performing hydrothermal treatment of these materials for a total of 15 h (same hydrothermal treatment time as used in the synthesis of HT_5-HSO_3-MCN). This suggests a lack of correlation between such hydrothermal treatment and catalytic activity, and effectively rules out, therefore, hydrolytic ring-opening of lactones on the carbon surface during hydrothermal treatment as being key for catalysis at the active sit.[29,30] In addition, we performed recycling experiments with catalyst HT_1-HSO_3-MCN. These experiments were performed by treating HT_1-HSO_3-MCN with extract solution followed by xylose release via hydrolysis catalysis. Afterward, the HT_1-HSO_3-MCN was regenerated and recycled using a brief regenerative wash (10 mg of catalyst was washed with 5 mL of 0.1 M NaOH in 50:50 v/v EtOH/H_2O, 5 mL of EtOH, 20 mL of deionized water, 3 mL of 4 M HCl, and 30 mL of deionized water, and dried before reuse for xylan hydrolysis in *Miscanthus* xylan extract), for a period of up to five recycles. Results shown in Figure S11 of the Supporting Information demonstrate a lack of catalyst deactivation for the five cycles investigated, though there is a slight deactivation between the first and the second recycle, which can be ascribed to the minor leaching of sulfonic acid sites observed in HT_1-HSO_3-MCN (vide supra). No such decrease was observed during recycling of catalyst HT_5-HSO_3-MCN, when using a similar procedure (Supporting Information Figure S12).

ATR-FTIR spectroscopy of all catalysts in Figure 2 was performed, and these spectra are shown in Figure 3. While catalyst COOH-MCN shows a prominent band as expected at 1725 cm^{-1} corresponding to carboxylic acid functionality, HT_5-

dx.doi.org/10.1021/cs400939p | *ACS Catal.* 2014, 4, 302−310

HSO_3-MCN lacks intensity altogether in this region (see Supporting Information for an enlarged representation of this spectral window for all catalysts). Our comparative catalytic data on various materials emphasize (i) a lack of evident correlation between carboxylic-acid content within the functionalized MCN material and hydrolysis catalysis, when comparing COOH-MCN (carboxylic-acid band in ATR-FTIR spectrum of Figure 3) and HT_5-HSO_3-MCN (lack of carboxylic-acid band in ATR-FTIR spectrum of Figure 3), both of which show similar xylan hydrolysis catalytic activity, and (ii) a lack of directly proportional correlation between phenolic OH content within the functionalized MCN material and hydrolysis catalysis, when comparing materials HT_5-HSO_3-MCN and untreated MCN (see Supporting Information). However, there is clearly a correlation with phenolic weak-acid site density and xylan hydrolysis catalysis activity, when comparing catalysts HT_5-HSO_3-MCN and untreated MCN, as described above. From this perspective, we hypothesize that the active sites responsible for observed hydrolysis catalysis may consist of that fraction of weak-acid sites that is expressed in a high local density on the surface, which may be present in either pockets or nests and at defect sites. For such organized weak-acid sites consisting of phenolic OH groups, hydrogen bonding may lower pK_a values of the organized OH groups akin to phenomena observed on calixarene macrocycles and defect sites on silica surfaces.[31] Previously, we have shown the latter to catalyze the hydrolysis of chemisorbed glucan polysaccharides on inorganic-oxide surfaces, with a rate that was proportional to the number density of weak-acid OH defect sites (i.e., the hydrolysis rate per grafted site on the chemisorbed grafted glucan was proportional to the OH-defect site density on the inorganic-oxide surface[4]). Based on the hypothesis above, the catalyst-synthesis challenge for the future becomes how to synthesize carbon materials with a higher local density of weak-acid defect sites. In the inorganic-oxide systems described above, this could be accomplished by switching from silica to alumina.[4]

In conclusion, we have demonstrated that catalytic material HT_5-HSO_3-MCN can hydrolyze (1→4)-β-D-xylan into xylose with significant yield of 74% at a buffered pH of 3.9, corresponding to that of xylan hemicellulose extract from *Miscanthus* biomass. This provides a rigorous demonstration of a weak-acid-catalyzed hydrolysis of a (1→4)-β-D-xylan and paves the way for highly active systems for biomass depolymerizations based on similar mechanisms, which employ adsorption and hydrolysis of confined polysaccharides on a weak acid-site surface catalyst.

■ ASSOCIATED CONTENT

Supporting Information

Further details are given in Figures S1−S12. This material is available free of charge via the Internet at http://pubs.acs.org.

■ AUTHOR INFORMATION

Corresponding Authors

*E-mail: cedricchung@berkeley.edu (P.-W.C.).
*E-mail: katz@cchem.berkeley.edu (A.K.).

Notes

The authors declare no competing financial interest.

■ ACKNOWLEDGMENTS

This work was supported by the Energy Bioscience Institute. The authors are grateful to Ms. Younjue Bae for conducting the catalyst recyclability studies described within the manuscript.

■ REFERENCES

(1) Binder, J. B.; Raines, R. T. *Proc. Natl. Acad. Sci.* **2010**, *107* (10), 4516−4521.
(2) Gazit, O. M.; Charmot, A.; Katz, A. *Chem. Commun.* **2010**, *47* (1), 376−378.
(3) Gazit, O. M.; Katz, A. *Langmuir* **2012**, *28* (1), 431−437.
(4) Gazit, O. M.; Katz, A. *J. Am. Chem. Soc.* **2013**, *135* (11), 4398−4402.
(5) Chung, P.-W.; Charmot, A.; Gazit, O. M.; Katz, A. *Langmuir* **2012**, *28* (43), 15222−15232.
(6) Mäki-Arvela, P. i.; Salmi, T.; Holmbom, B.; Willför, S.; Murzin, D. Y. *Chem. Rev.* **2011**, *111* (9), 5638−5666.
(7) Fanta, G. F.; Abbott, T. P.; Herman, A. I.; Burr, R. C.; Doane, W. M. *Biotechnol. Bioeng.* **1984**, *26* (9), 1122−1125.
(8) González, G.; López-Santín, J.; Caminal, G.; Solà, C. *Biotechnol. Bioeng.* **1986**, *28* (2), 288−293.
(9) Neureiter, M.; Danner, H.; Thomasser, C.; Saidi, B.; Braun, R. *Appl. Biochem. Biotechnol.* **2002**, *98−100*, 49−58.
(10) Lloyd, T. A.; Wyman, C. E. *Bioresour. Technol.* **2005**, *96* (18), 1967−1977.
(11) Mussatto, S. I.; Roberto, I. C. *J. Sci. Food Agric.* **2005**, *85* (14), 2453−2460.
(12) Kobayashi, H.; Yabushita, M.; Komanoya, T.; Hara, K.; Fujita, I.; Fukuoka, A. *ACS Catal.* **2013**, 581−587.
(13) de Clippel, F.; Dusselier, M.; Van Rompaey, R.; Vanelderen, P.; Dijkmans, J.; Makshina, E.; Giebeler, L.; Oswald, S.; Baron, G. V.; Denayer, J. F. M.; Pescarmona, P. P.; Jacobs, P. A.; Sels, B. F. *J. Am. Chem. Soc.* **2012**, *134* (24), 10089−10101.
(14) Kobayashi, H.; Ohta, H.; Fukuoka, A. *Catal. Sci. Technol.* **2012**, *2* (5), 869−883.
(15) Demma Carà, P.; Pagliaro, M.; Elmekawy, A.; Brown, D. R.; Verschuren, P.; Shiju, R. N.; Rothenberg, G. *Catal. Sci. Technol.* **2013**, *3*, 2057−2061.
(16) Rinaldi, R.; Meine, N.; vom Stein, J.; Palkovits, R.; Schüth, F. *ChemSusChem* **2010**, *3* (2), 266−276.
(17) Bazuła, P. A.; Lu, A.-H.; Nitz, J.-J.; Schüth, F. *Microporous Mesoporous Mater.* **2008**, *108* (1−3), 266−275.
(18) Kim, T.-W.; Chung, P.-W.; Slowing, I. I.; Tsunoda, M.; Yeung, E. S.; Lin, V. S.-Y. *Nano Lett.* **2008**, *8* (11), 3724−3727.
(19) Kim, T.-W.; Chung, P.-W.; Lin, V. S.-Y. *Chem. Mater.* **2010**, *22* (17), 5093−5104.
(20) Suganuma, S.; Nakajima, K.; Kitano, M.; Yamaguchi, D.; Kato, H.; Hayashi, S. *J. Am. Chem. Soc.* **2008**, *130* (38), 12787−12793.
(21) Onda, A.; Ochi, T.; Yanagisawa, K. *Green Chem.* **2008**, *10* (10), 1033.
(22) Sluiter,A.; Hames, B.; Ruiz, R.; Scarlata, C.; Sluiter, J.; Templeton, D.; Crocker, D. Determination of Structural Carbohydrates and Lignin in Biomass. In *Laboratory Analytical Procedure*; National Renewable Energy Laboratory: Golden, CO, 2008.
(23) Mo, X.; López, D. E.; Suwannakarn, K.; Liu, Y.; Lotero, E.; Goodwin, J.; James, G.; Lu, C. *J. Catal.* **2008**, *254* (2), 332−338.
(24) Liu, X.-Y.; Huang, M.; Ma, H.-L.; Zhang, Z.-Q.; Gao, J.-M.; Zhu, Y.-L.; Han, X.-J.; Guo, X.-Y. *Molecules* **2010**, *15* (10), 7188−7196.
(25) Ferrari, A. C.; Robertson, J. *Phys. Rev. B* **2000**, *61* (20), 14095−14107.
(26) Somerville, C.; Youngs, H.; Taylor, C.; Davis, S. C.; Long, S. P. *Science* **2010**, *329* (5993), 790−792.
(27) Haffner, F. B.; Mitchell, V. D.; Arundale, R. A.; Bauer, S. *Cellulose* **2013**, *20* (4), 1629−1637.
(28) Yang, B.; Dai, Z.; Ding, S.-Y.; Wyman, C. E. *Biofuels* **2011**, *2* (4), 421−450.
(29) Stein, A.; Wang, Z.; Fierke, M. A. *Adv. Mater.* **2009**, *21* (3), 265−293.

(30) Fanning, P. E.; Vannice, M. A. *Carbon* **1993**, *31* (5), 721−730.
(31) Bass, J. D.; Solovyov, A.; Pascall, A. J.; Katz, A. *J. Am. Chem. Soc.* **2006**, *128* (11), 3737−3747.